Quasifree-scattering model for the imaginary part of the optical potential for electron scattering

Grażyna Staszewska, David W. Schwenke, Devarajan Thirumalai,* and Donald G. Truhlar
Deparment of Chemistry, University of Minnesota, Minneapolis, Minnesota 55455
(Received 28 March 1983)

A relatively simple nonempirical formula for the imaginary part of the optical potential for electron scattering is derived from a quasifree-scattering model with Pauli blocking in which the target is treated as a free-electron gas. The resulting absorption potential is local and energy dependent and is a function of the electron density of the target. This model is tested for electron-helium and electron-neon scattering at 30—3000 eV. For these tests the real part of the potential is also approximated by a local expression, which is partitioned into static, exchange, and polarization terms. Reasonably good agreement with experimental data is obtained for the elastic integral, absorption, and elastic differential cross sections.

I. INTRODUCTION

In 1948, Goldberger, following up on a physical model suggested by Serber,[1] calculated the mean free path of a nucleon in a nucleus by treating the nucleus as a degenerate Fermi gas and considering the nucleon-nucleon scattering to be the result of individual nucleon-nucleon collisions.[2] An important element in this model is the role of the Pauli principle in restricting the momentum space available to the products of a collision.[1-3] The model has been successively refined by many workers. A more systematic approach along these lines may be derived from the impulse approximation[4] and the multiple-scattering series[5] in which the many-body transition amplitude T for nucleon-nucleus scattering is approximated in terms of the two-body transition amplitude t for the nucleon-nucleon scattering. Then, if one assumes that only the forward-scattering amplitude $t(0)$ is important, one may recover the original kinetic-theory argument in terms of binary-collision total cross sections.[6] The relation of the two methods is provided by the optical theorem which relates the imaginary part of $t(0)$ to the total scattering cross section for binary collisions.[7] The forward scattering approximation is sometimes called the frivolous model to emphasize the simplicity that follows from the neglect of many-body effects. We will call the Goldberger approximation, which involves differential cross sections in order to satisfy the Pauli-principle restrictions, the quasifree-scattering model. This emphasizes that the differential cross sections for the two-body collisions are calculated as if the constituents of the target were free particles. The target properties enter only through initial conditions of the binary collisions, which are determined by the spatial and momentum density distributions for the target particles, and through the Pauli-principle restrictions on allowed final states of the binary collisions.

It is the purpose of the present paper to report an application of the quasifree-scattering approximation to atomic physics. In particular, we apply this model to calculate the absorption potential for intermediate-energy and high-energy electron scattering by the rare gases He and Ne. In this application, unlike the nuclear applications where the binary collisions are governed by the strong interaction, the binary collisions are governed by a known force law, the Coulomb potential. This means that the binary cross sections need not be modeled phenomenologically. It also means that the binary-collision total cross sections are infinite. Thus the Pauli-principle restrictions are essential for the model to yield a finite mean free path and absorption potential. Finally, the differential cross section for Coulomb scattering is nonisotropic; as compared to the isotropic cross section assumed in the nuclear applications, this means that the differential cross section is not totally determined by the integral cross section, and it complicates the integrations considerably.

II. THEORY

In this paper we seek to approximate the absorption potential for electron scattering by an energy-dependent function $V^A(\vec{r},E)$ where $\vec{r}$ is the coordinate of the scattering electron and E is its impact energy. For electron scattering by spherical atoms $V^A(\vec{r},E)$ will depend on the magnitude of $\vec{r}$ and not on the angular coordinates; however, the derivation is more general and it applies equally well to molecular targets or surfaces. The coordinate frame in which the target is at rest will be called the laboratory frame, and the coordinate frame in which the center of mass of a pair of electrons (the scattering electron and a target electron) is at rest will be called the binary-collision frame. In transforming between these frames we assume that the nucleus is infinitely heavy compared to the scattering electron; this is an excellent approximation for all targets of interest.

For a local imaginary potential such as iV^A the absorption probability per unit time is $-2V^A/\hbar$.[8] Thus V^A should be negative. In kinetic theory the absorption probability per unit time for an electron of local kinetic energy $T_{\rm loc}$ and mass m, passing through a gas of density ρ, with a binary-collision cross section $\bar{\sigma}_b$ for absorption-

producing events, is $(2T_{\rm loc}/m)^{1/2}\rho\bar{\sigma}_b$. In the present application, $T_{\rm loc}$ depends on the magnitude p of the incident momentum and on $\vec{r}$, the density is the target electron density, which depends on $\vec{r}$, and $\bar{\sigma}_b$ depends on both ρ and p because of the Pauli-principle restrictions. Hence[6,9,10]

$$V^A(\vec{r},E)=\frac{-\hbar\rho(\vec{r})[T_{\rm loc}(p,\vec{r})]^{1/2}\bar{\sigma}_b(k_F[\rho(\vec{r})],p)}{(2m)^{1/2}}\ , \tag{1}$$

where k_F is the Fermi momentum given by

$$k_F(\rho(\vec{r}))=[3\pi^2\rho(\vec{r})]^{1/3}\hbar \tag{2}$$

and

$$E=p^2/2m\ . \tag{3}$$

As discussed by Goldberger, but in a more explicit notation,

$$\bar{\sigma}_b(k_F,p)=\frac{1}{p}\int d\vec{k}\,N(\vec{k},k_F)\,|\,\vec{p}-\vec{k}\,|\times\int d\vec{g}\frac{d\sigma_b(p_0,\hat{p}_0\cdot\hat{p}_f)}{d\Omega}\times\frac{1}{p_0^2}\delta(p_0-p_f)\Theta(p',k',k_F)\ , \tag{4}$$

where $N(\vec{k},k_F)$ is the density per target electron in momentum space, $\vec{p}$ and $\vec{k}$ are the laboratory-frame momenta of the incident and target electrons before the collision, $\vec{p}\,'$ and $\vec{k}\,'$ are the final values, $\vec{p}_0$ and $\vec{p}_f$ are the initial and final momenta of the scattering electron in the binary-collision frame, $\vec{g}$ is the momentum transfer

$$\vec{g}=\vec{p}\,'-\vec{p} \tag{5a}$$

$$=\vec{p}_f-\vec{p}_0\ , \tag{5b}$$

$d\sigma_b/d\Omega$ is the differential cross section for binary collisions, and Θ is a function that is unity for Pauli-allowed final states of the binary collision and zero for Pauli-blocked collisions. If the electronic distribution of the target is modeled as a quasidegenerate Fermi gas then

$$N(\vec{k},k_F)=\begin{cases}N_k(k_F), & k\le k_F \quad (6a)\\ 0, & k>k_F \quad (6b)\end{cases}$$

where

$$N_k(k_F)=3/(4\pi k_F^3)\ . \tag{7}$$

In nuclear-physics applications the Pauli-blocking function is usually assumed to be

$$\Theta(p',k',k_F)=H(p'-k_F)H(k'-k_F)\ , \tag{8}$$

where $H(x)$ is the Heaviside unit-step function. This gives a finite result for the nuclear-physics case, namely, constant $d\sigma_b/d\Omega$, but for Coulomb scattering it leads to an infinite cross section. A physically acceptable model for this case is obtained by taking account of the finite energy gap between the highest occupied orbital in the ground-state target and the lowest unoccupied orbital. This leads to a more stringent Pauli-blocking function given by

$$\Theta(p',k',k_F)=H(k'^2-k_F^2-w)H(p'-k_F)\ , \tag{9}$$

where

$$w=2m\Delta \tag{10}$$

and Δ is the energy gap between the target ground state and lowest excited electronic state. Equation (8) has the interpretation that neither electron involved in the binary collision may be scattered into the occupied Fermi sea, but Eq. (9) involves an additional restriction that the final energy of the originally bound electron must exceed the energy of the highest occupied state by at least the energy gap Δ. It is more convenient to use the quantity w defined by (10) in the subsequent derivation.

The Coulomb scattering cross section for distinguishable particles is given by the Rutherford formula. For identical particles we should use the quantum-mechanical Mott formula but this leads to a complicated angle-dependent, energy-dependent correction. Because of the Pauli restrictions, the forward and much of the near-forward scattering is excluded; hence we seek a good approximation for sideways scattering. For $\theta=\pi/2$ the quantum effect is to reduce the differential cross sections by exactly a factor of 2 at all energies.[11] In this work we use the sideways approximation of simply dividing the Rutherford formula by 2 at all angles and energies. This yields

$$\frac{d\sigma_b(p_0,\hat{p}_0\cdot\hat{p}_f)}{d\Omega}=\frac{2}{g^4}\ . \tag{11}$$

Substituting (6), (9), and (11) into (4) and using

$$\delta(f(x))=\left|\frac{df}{dx}\right|^{-1}_{x=x_0}\delta(x-x_0),\quad f(x_0)=0 \tag{12}$$

yields

$$\bar{\sigma}_b(k_F,p)=\frac{8N_k(k_F)}{p}\int d\vec{g}\int d\vec{k}\,H[k'-(k_F^2+w)^{1/2}]H(p'-k_F)g^{-4}H(k_F-k)\delta(p_0^2-p_f^2) \tag{13a}$$

$$=\frac{8N_k(k_F)}{p}\int d\vec{g}\,H(g^2+p^2+2\vec{g}\cdot\vec{p}-k_F^2)g^{-4}I_1(\vec{p},\vec{g})\ , \tag{13b}$$

where

$$I_1(\vec{p},\vec{g})=\int d\vec{k}\,H(g^2+k^2-2\vec{g}\cdot\vec{k}-k_F^2-w)H(k_F^2-k^2)\delta(p_0^2-p_f^2)\ . \tag{14}$$

The integral in (14) is most easily performed using cylindrical coordinates k_R, k_Z, k_Φ for $\vec{k}$ with the k_Z axis antiparallel to $\vec{g}$. The k_Φ integral gives 2π and the k_Z integral may be evaluated to yield

$$I_1(\vec{p},\vec{g})=(2\pi/g)\int dk_R k_R H(k_R^2+(k_{Z0}+g)^2-k_F^2-w)H(k_F^2-k_R^2-k_{Z0}^2)\ , \tag{15}$$

where

$$k_{Z0}=-g-\vec{p}\cdot\hat{g}\ . \tag{16}$$

Evaluating the k_R integral then gives

$$I_1(\vec{p},\vec{g})=\frac{\pi}{g}H(-g^2-2\vec{g}\cdot\vec{p}-w)H(k_F^2-g^{-2}(g^2+\vec{p}\cdot\vec{g})^2)\{k_F^2-k_{Z0}^2+H(k_F^2+w-(k_{Z0}+g)^2)[(k_{Z0}+g)^2-k_F^2-w]\}\ . \tag{17}$$

Next we substitute (17) into (13b) and use (5a) to change the integration variable to $\vec{p}\,'$. We use spherical coordinates (p',η,ϕ) for $\vec{p}\,'$ where the p_Z' axis is along $\vec{p}$. The ϕ integral yields 2π, and this simplifies the cross section to

$$\bar{\sigma}(k_F,p)=\frac{16\pi^2 N_k(k_F)}{p}\int dp'p'^2 H(p'^2-k_F^2)H(p^2-p'^2-w)$$
$$\times\int dy H(k_F^2-f(p,p',y))\frac{1}{(p'^2+p^2-2pp'y)^{5/2}}$$
$$\times\{k_F^2-f(p,p',y)+H(k_F^2+w-f(p',p,y))[f(p',p,y)-k_F^2-w]\}\ , \tag{18}$$

where

$$f(p,p',y)=\frac{(-p'^2+pp'y)^2}{p'^2+p^2-2pp'y} \tag{19}$$

and

$$y=\cos\eta\ . \tag{20}$$

Evaluating the y integral yields

$$\bar{\sigma}(k_F,p)=\frac{64\pi^2 N_k(k_F)}{15p}\int dp'p' H(p'^2-k_F^2)H(p^2-p'^2-w)\left[\frac{5\xi+4}{k_F\xi^3}+H(k_F^2+w-p^2+p'^2)\frac{(1-\xi)^{1/2}(\xi^2+3\xi-4)}{(k_F^2+w)^{1/2}\xi^3}\right], \tag{21}$$

where

$$\xi=(p^2-p'^2)/k_F^2 \tag{22}$$

and

$$\zeta=(p^2-p'^2)/(k_F^2+w)\ . \tag{23}$$

Evaluating the final integral then yields

$$\bar{\sigma}(k_F,p)=\frac{32\pi^2 N_k(k_F)}{15p^2}H(p^2-k_F^2-w)\left[\frac{5k_F^3}{w}-\frac{k_F^3(5p^2-3k_F^2)}{(p^2-k_F^2)^2}+H(2k_F^2+w-p^2)\frac{2(2k_F^2+w-p^2)^{5/2}}{(p^2-k_F^2)^2}\right]. \tag{24}$$

Notice that the dependence of $\bar{\sigma}_b$ on ρ is implicit through $k_F[\rho(\vec{r})]$, and $\bar{\sigma}_b$ also depends on the energy gap through w.

The final expression for the absorption potential is obtained by combining equations (1)—(3), (7), and (24). Notice that the result becomes infinite for p greater than k_F if the gap is zero. Our choice of gap makes $V^A(\vec{r},E)$ have the correct threshold.

III. CALCULATIONS

The whole optical potential is approximated as

$$V^{\rm opt}(\vec{r},E)=V^R(\vec{r},E)+iV^A(\vec{r},E)\ , \tag{25}$$

where the real part V^R is further partitioned into static (S), exchange (E), and polarization (P) terms[12]:

$$V^R(\vec{r},E)=V^S(\vec{r})+V^E(\vec{r},E)+V^P(\vec{r},E)\ . \tag{26}$$

The static part is obtained from a fit to the results of Hartree-Fock calculations, and the exchange term is calculated by the semiclassical-exchange approximation[13] as a function of the unperturbed Hartree-Fock density[14] and the Hartree-Fock static potential. The polarization term for most of the calculations is a spline fit to results[15,16]

TABLE I. Parameter $c(E)$ of the SEPaAρ potential (in a.u.).

E (eV)	He	Ne
100	1.411 03	0.386 29
1000	1.416 96	0.704 97

obtained in the adiabatic approximation by the finite-field variational method[17] using Hartree-Fock wave functions with an extended basis set including diffuse functions. Notice that, in general, as written in (26), the V^P term may be energy-dependent, but in the adiabatic approximation it is independent of energy. The absorption potential is evaluated using the formula derived in Sec. II; this requires the density and the local kinetic energy. For the former we used the unperturbed Hartree-Fock density; the latter was modeled using the static and semiclassical-local-exchange potentials, i.e.,

$$T_{\rm loc}(\vec{r},E)=E-V^S(\vec{r})-V^E(\vec{r},E)\ . \tag{27}$$

The calculations with the potential model just described will be called SEPaA or SEPaAf, where the capital letters denote the four terms in the potential, "a" denotes adiabatic polarization, and "f" denotes the quasifree-scattering approximation for absorption. We will also report a few calculations with other polarization or absorption models or with one of these terms neglected. In the SEPlkeAf model the adiabatic polarization potential $V^{\rm Pa}$ is replaced by the local-kinetic-energy semiclassical polarization approximation,[18] i.e.,

$$V^{\rm Plke}(\vec{r},E)=[1+T_{\rm loc}(\vec{r},E)/\Delta_{\rm av}]^{-1}V^{\rm Pa}(\vec{r})\ , \tag{28}$$

where $T_{\rm loc}$ is given by (27) and $\Delta_{\rm av}$ is an average excitation energy. The SEPleAf model involves the low-energy semiclassical polarization approximation,[18] i.e.,

$$V^{\rm Ple}(\vec{r},E)=\{1-[V^S(\vec{r})+V^E(\vec{r},E)]/\Delta_{\rm av}\}^{+1}V^{\rm Pa}(\vec{r})\ . \tag{29}$$

In the SEAf model the polarization potential is neglected entirely. In the SEPaAρ model, we tested the effect of using a different shape for the absorption potential. We took the absorption potential as

$$V^{A\rho}(\vec{n},E)=-c(E)\rho(\vec{r})\ , \tag{30}$$

where $c(E)$ is an empirical constant that we adjusted to

TABLE II. Cross sections (a_0^2) and differential cross sections (a_0^2/sr) at four scattering angles for various potentials.

Potential	$\sigma_{\rm el}$	$\sigma_{\rm abs}$	$\sigma_{\rm tot}$	$\sigma_{\rm el}^m$	$d\sigma_{\rm el}/d\Omega$ 2°	10°	60°	120°
				He at 100 eV				
SEPaA	2.82	1.93	4.75	0.827	3.61	2.49	0.177	0.0296
SEPleA	2.44	1.92	4.35	0.703	3.32	2.24	0.148	0.0254
SEPlkeA	1.98	1.90	3.88	0.690	1.54	1.33	0.147	0.0270
SEA	1.84	1.89	3.73	0.676	1.21	1.11	0.143	0.0273
SEPaAρ	2.23	1.89	4.12	0.581	3.13	2.09	0.142	0.0157
SEPa	3.13	0	3.13	1.14	3.68	2.47	0.224	0.0506
				He at 1000 eV				
SEPaA	0.267	0.446	0.713	0.0155	2.61	0.680	0.002 18	0.000 218
SEPleA	0.219	0.445	0.664	0.0135	2.29	0.551	0.002 08	0.000 223
SEPlkeA	0.153	0.444	0.598	0.0132	0.731	0.374	0.002 13	0.000 223
SEA	0.151	0.444	0.596	0.0132	0.700	0.367	0.002 13	0.000 223
SEPaAρ	0.269	0.616	0.885	0.0145	2.64	0.700	0.001 90	0.000 188
SEPa	0.286	0	0.286	0.0200	2.70	0.696	0.003 16	0.000 349
				Ne at 100 eV				
SEPaA	7.49	4.69	12.2	3.66	10.9	7.89	0.172	0.141
SEPleA	7.14	4.65	11.8	3.39	10.4	7.44	0.167	0.151
SEPlkeA	5.73	4.65	10.4	3.33	6.09	5.17	0.141	0.120
SEA	6.26	4.59	10.9	3.27	6.22	5.46	0.153	0.147
SEPaAρ	6.60	3.01	9.60	2.48	9.52	6.56	0.302	0.0662
SEPa	9.43	0	9.43	6.60	10.0	6.89	0.413	0.272
				Ne at 1000 eV				
SEPaA	1.60	1.90	3.51	0.0914	13.9	4.53	0.0129	0.001 68
SEPleA	1.41	1.89	3.30	0.0845	12.2	3.91	0.0121	0.001 70
SEPlkeA	1.24	1.89	3.13	0.0839	7.35	3.56	0.0123	0.001 70
SEA	1.23	1.89	3.12	0.0838	7.23	3.54	0.0123	0.001 70
SEPaAρ	1.65	1.31	2.96	0.0876	14.2	4.57	0.0138	0.000 776
SEPa	2.35	0	2.35	0.308	15.6	5.23	0.0529	0.0107

TABLE III. Theoretical (SEPaA and SEPlkeA) and experimental (Refs. 19, 26, 27, and 30) cross sections for He.

E (eV)	SEPaA	SEPlkeA	Ref. 26	Refs. 19 and 27	Ref. 30
			σ_{el} (a_0^2)		
30	9.148	7.744	7.54	7.99	8.46
50	5.804	4.476	4.51	4.95	5.21
100	2.817	1.984	2.00	2.18	2.36
200	1.277	0.839	0.88	0.98	1.07
400	0.627	0.385	0.41	0.44	0.43
700	0.374	0.220	0.23	0.236	
800	0.330	0.192	0.21		
1000	0.267	0.153	0.15	0.149	
3000	0.0914	0.0507		0.048	
			σ_{abs} (a_0^2)		
30	0.370	0.372		0.815	
50	1.295	1.279		1.52	
100	1.934	1.898		1.89	
200	1.652	1.629		1.65	
400	1.024	1.015		1.16	
700	0.623	0.620		0.80	
800	0.550	0.548		0.73	
1000	0.446	0.444		0.61	
3000	0.153	0.154		0.25	
			σ_{tot} (a_0^2)		
30	9.518	8.116	8.36	8.80	
50	7.099	5.755	6.04	6.47	
100	4.751	3.881	3.89	4.07	
200	2.929	2.467	2.53	2.63	
400	1.651	1.399	1.57	1.61	
700	0.997	0.839	1.04	1.04	
800	0.880	0.740	0.95		
1000	0.713	0.598	0.76	0.76	
3000	0.245	0.204		0.31	
			σ_{el}^m (a_0^2)		
30	6.623	5.783	5.38		6.00
50	3.018	2.550	2.51		2.93
100	0.827	0.690	0.75		0.93
200	0.205	0.169	0.22		0.29
400	0.0630	0.0520			0.079
700	0.0272	0.0228			
800	0.0221	0.0187			
1000	0.0155	0.0132			
3000	0.002 47	0.002 17			
			$d\sigma_{el}/d\Omega$ (a_0^2/sr) at $\theta=20°$		
30	2.269	1.639	1.88		
50	2.100	1.384	1.56		
100	1.529	0.966	0.90	0.93	
200	0.874	0.564	0.49	0.53	
400	0.433	0.290		0.29	
700	0.222	0.157		0.154	
800	0.186	0.133			
1000	0.135	0.0989		0.098	
3000	0.0207	0.0177		0.018	

make the absorption cross section agree wth experiment.[19,20] The resulting values of $c(E)$ are given in Table I. Finally, in the SEPa model, we neglect the absorption potential.

Since most results in this paper are for the Af model for absorption, we further abbreviate Af by A in tables and figures.

For the energy gaps in the absorption potential we used

TABLE IV. Theoretical (SEPaA) and experimental (Refs. 20 and 27–29) cross sections for Ne.

E (eV)	SEPaA	Refs. 20 and 27	Ref. 29	Ref. 28
		σ_{el} (a_0^2)		
30	10.71	11.3	12.9	
40	10.70	10.7		
50	10.26	10.8	11.2	
70	9.076	9.99	10.1	
100	7.493	8.74	7.96	8.55
200	4.619	4.99		4.92
400	2.652	3.22		3.24
1000	1.604	1.63		
3000	0.774	0.75		
		σ_{abs} (a_0^2)		
30	1.236	0.75	>1.01	
40	2.374	1.35		
50	3.208	1.85	>1.99	
70	4.166	2.53		
100	4.693	2.92	>2.79	
200	4.517	2.99		
400	3.503	2.30		
1000	1.902	1.31		
3000	0.783	0.55		
		σ_{tot} (a_0^2)		
30	11.95	12.1	13.6	
40	13.07	12.1		
50	13.47	12.7	13.0	
70	13.24	12.5	12.6	
100	12.19	11.7	10.9	
200	9.136	7.98		
400	6.155	5.51		
1000	3.506	2.94		
3000	1.556	1.30		
		σ_{el}^m (a_0^2)		
30	9.305		10.5	
40	8.834			
50	7.849		8.57	
70	5.796		5.93	
100	3.659		4.71	4.54
200	1.174			2.10
400	0.260			0.88
1000	0.0914			
3000	0.0225			
		$d\sigma_{el}/d\Omega$ (a_0^2/sr) at $\theta=20°$		
30	1.810		2.18	
40	2.783			
50	3.520		3.24	
70	4.307		4.27	
100	4.534	4.15	3.70	4.48
200	3.524	2.75		2.50
400	1.991	1.84		1.96
1000	0.787	0.91		
3000	0.173	0.28		

19.9181 eV for He and 16.6194 eV for Ne.[21] For the average excitation energies in the semiclassical polarization potentials we used 25.42 eV for He and 25.27 eV for Ne.[22] Figures 1 and 2 show absorption potentials computed by the quasifree-scattering model for He and Ne, respectively.

TABLE V. Differential cross sections (a_0^2/sr) for electron-He scattering at $E=800$ eV.

θ (deg)	SEPaA	SEPlkeA	Expt.[a]
10	0.814	0.433	0.46
20	0.186	0.133	0.15
30	0.0499	0.0404	0.051
50	0.006 69	0.006 25	0.0093
70	0.001 79	0.001 76	0.0029
90	0.000 725	0.000 735	0.0013
110	0.000 389	0.000 399	0.000 80
130	0.000 225	0.000 262	0.000 49
150	0.000 197	0.000 202	0.000 40

[a]Reference 31.

The complex phase shifts and the cross sections were calculated using methods discussed elsewhere.[23,24] To converge the partial-wave sums in the cross-section formulas we used l_{max} values in the range from 13 to 351; in some cases the high-l phase shifts were computed in the polarized Born approximation[25] with the asymptotic polarization potential. In all cases the results presented are well converged with respect to increasing l_{max} and, where applicable, with respect to increasing the l value at which we switched from numerical phase shifts to polarized Born ones for the asymptotic polarization potential.

IV. RESULTS

Table II compares cross sections computed with all six types of potential for two energies. The abbreviations

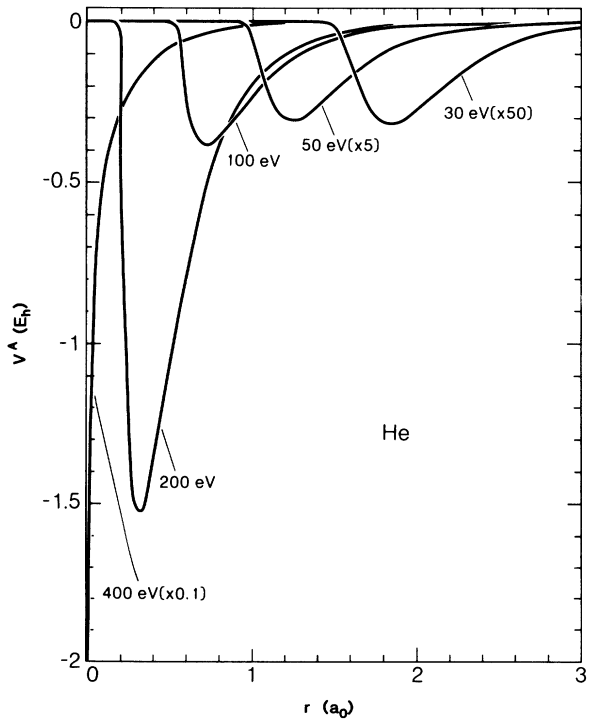

FIG. 1. Absorption potentials computed by the quasifree-scattering model for He.

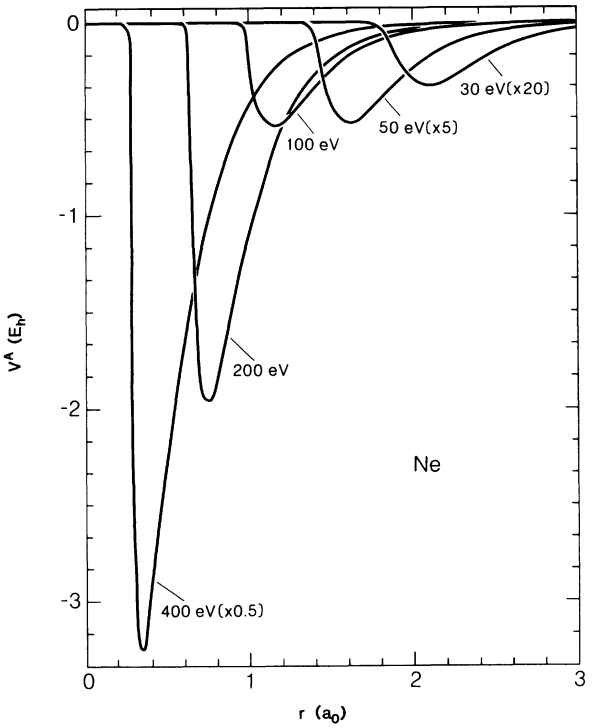

FIG. 2. Absorption potentials computed by the quasifree-scattering model for Ne.

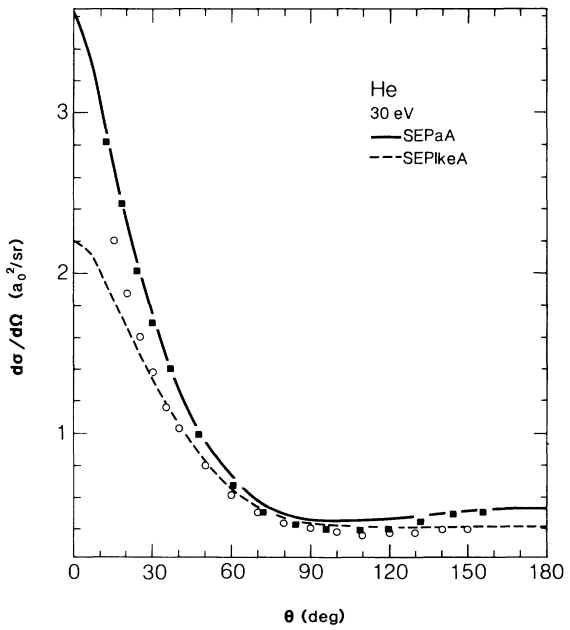

FIG. 3. Differential cross sections for He at 30 eV. In all the differential cross-section figures we use curves for theoretical results, with the potentials indicated in the figures, and symbols for the experimental results. We use the same convention for the symbols in all the figures: △, Gupta and Rees, Ref. 28; +, Kurepa and Vušković, Ref. 32; ▽, Williams and Crowe, Ref. 33; ×, Jansen *et al.*, Ref. 27; ◇, DuBois and Rudd, Ref. 34; ○ Register *et al.*, Ref. 26 and 29; ■, Shyn, Ref. 30.

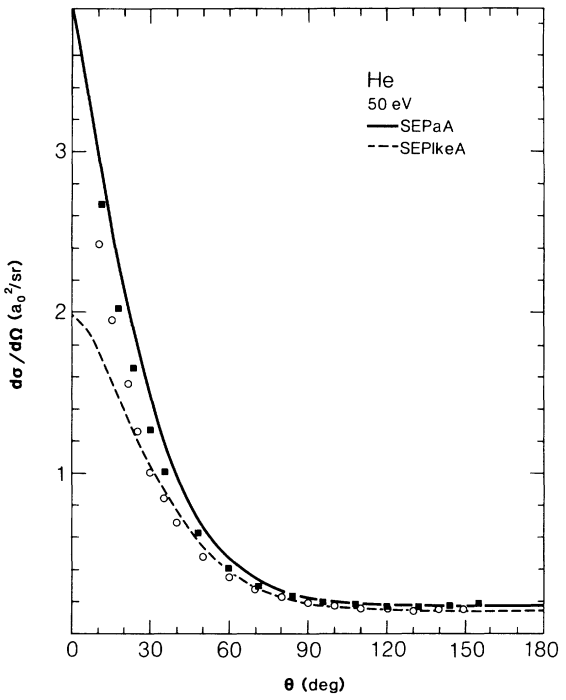

FIG. 4. Same as Fig. 3 except for 50 eV.

used for the cross sections are as follows: $d\sigma_{el}/d\Omega$, elastic differential cross section per unit solid scattering angle; σ_{el}, elastic integral cross section; σ_{el}^m, elastic momentum-transfer cross section; σ_{abs}, absorption cross section; and σ_{tot}, total scattering cross section, defined by

$$\sigma_{tot}=\sigma_{el}+\sigma_{abs} . \tag{31}$$

Tables III and IV give results for two potentials for He and for one potential for Ne as functions of energy; these tables also contain experimental results[19,20,26–30] for comparison. Table V and Figs. 3–16 compare differential cross sections to experiment.[26–34]

V. DISCUSSION

Figures 1 and 2 show that the present model leads to preferential absorption in the vicinity of the atomic surface or beyond at the lower impact energies, and that the peak moves to the nucleus as the energy is increased. At the lower energies the absorption potential has the shape

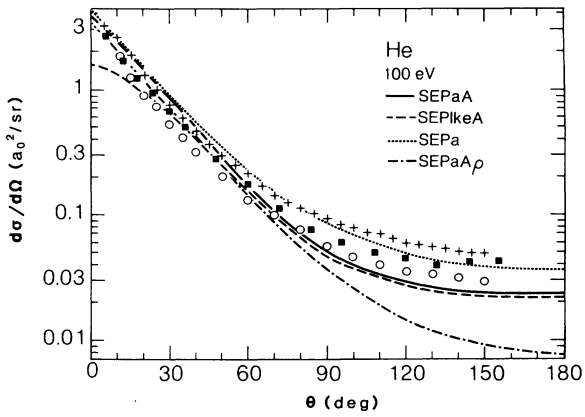

FIG. 5. Same as Fig. 3 except for 100 eV.

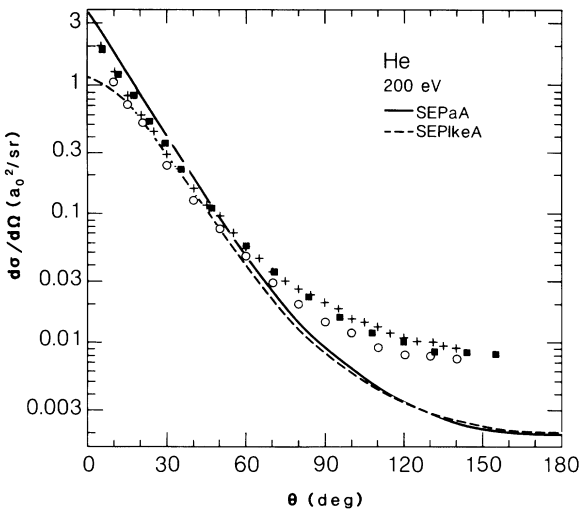

FIG. 6. Same as Fig. 3 except for 200 eV.

of the bottom of a French wine bottle. Wine-bottle absorption potentials are familiar in nuclear physics, where absorption is believed to be most probable at the nuclear surface. The absorption potentials of most models used in electron-atom scattering are peaked at the origin,[35–37] although McCarthy *et al.*[38] presented a series of reasonably successful calculations with a wine-bottle-shaped absorption potential that they adjusted to experimental data. In the present model a greater absorption probability at the atomic surface arises physically from the lower Fermi momenta in the outer low-density regions of the atom. According to the model, the Pauli blocking is less severe in regions of lower Fermi momentum. In order to test the significance of the surface absorption feature we replaced the Af absorption potential by the Aρ one, Eq. (30). The reason for using $\rho(\vec{r})$ is that it is the simplest nonsingular

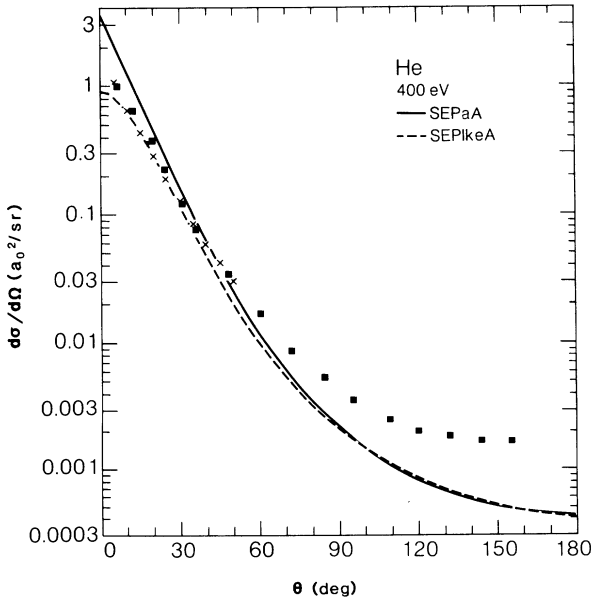

FIG. 7. Same as Fig. 3 except for 400 eV.

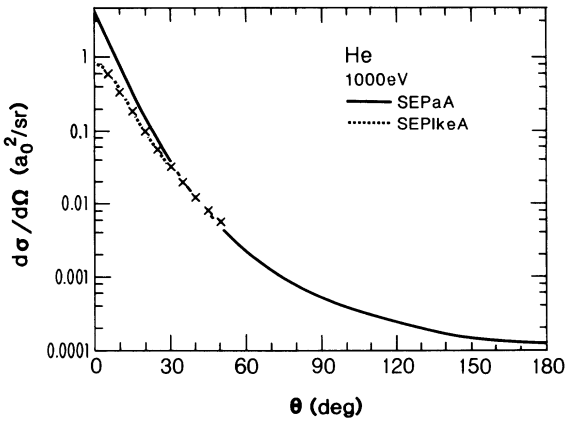

FIG. 8. Same as Fig. 3 except for 1000 eV.

function associated with the atom that is peaked at the nucleus, and, in fact, it represents the simplest possible binary-collision model in which the probability of absorption is simply proportional to the probability of finding an electron. Table II shows that for many properties of the cross sections the nonempirical Af model and the empirical Aρ model predict similar results. Figures 5 and 12 show, however, that the Aρ absorption potential predicts too little large-angle elastic scattering for He and Ne at 100 eV. In both cases the angle dependence of the elastic differential cross section is predicted much more accurately by the Af absorption potential than the Aρ one. Rather than explore nuclear-peaked absorption potentials further, we shall concentrate in the rest of this paper on testing the Af absorption potential to see if the quasifree-scattering model with Pauli blocking can provide a useful basis for accounting for flux loss from the elastic channel.

We also ask the following: Can we draw reasonably reliable conclusions about the absorption potential when the real polarization potential also has uncertainties? Several of the calculations in Table II were designed to answer this question. Comparison of the SEPaAf or SEPaAρ differential cross sections to the SEPa ones shows that the main effect of the absorption potential is to decrease the large-angle scattering. But comparison of the SEPaAf, SEPlkeAf, and SEPleAf differential cross sections at large

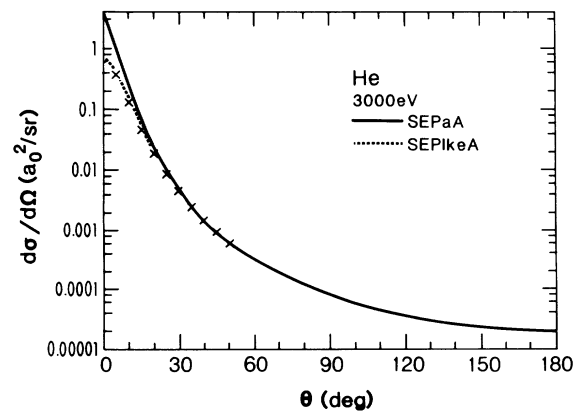

FIG. 9. Same as Fig. 3 except for 3000 eV.

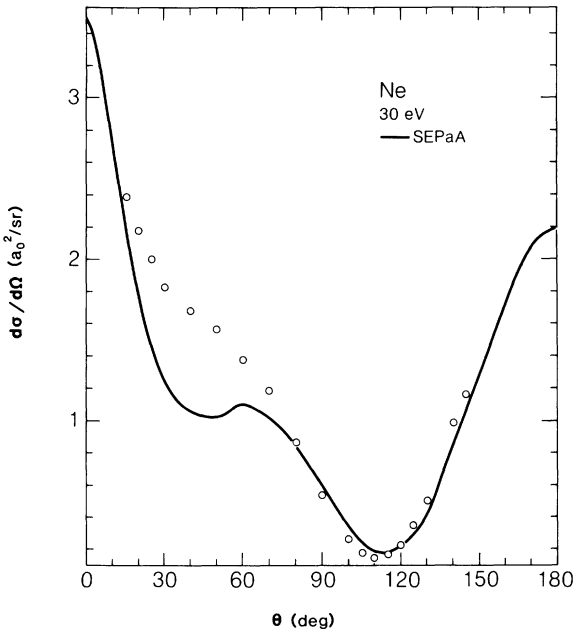

FIG. 10. Same as Fig. 3 except for Ne at 30 eV.

scattering angles shows that they are very similar. Changing the polarization potential also has only a small effect on σ_{abs}. Thus the two most important effects of V^A, namely, the absorption cross section and the lowering of the large-angle differential elastic cross section, are insensitive to the polarization potential. We conclude that the answer to the question posed at the beginning of this paragraph appears to be yes.

To test the new model for the absorption potential we will use the Pa and Plke polarization potentials for He and the Pa polarization potential for Ne. We know from previous work on He at 12–400 eV and on Ne at 10–700 eV that these potentials are reasonably adequate over wide energy ranges.[16,22,24,39,40] At still higher energies it might be more appropriate to use the SEAf model. However, as discussed above, our conclusions about σ_{abs} should be reasonably independent of the polarization potential. Additional calculations show that at high energy the effect of the polarization potential on $d\sigma_{el}/d\Omega$ is limited to very small scattering angles.

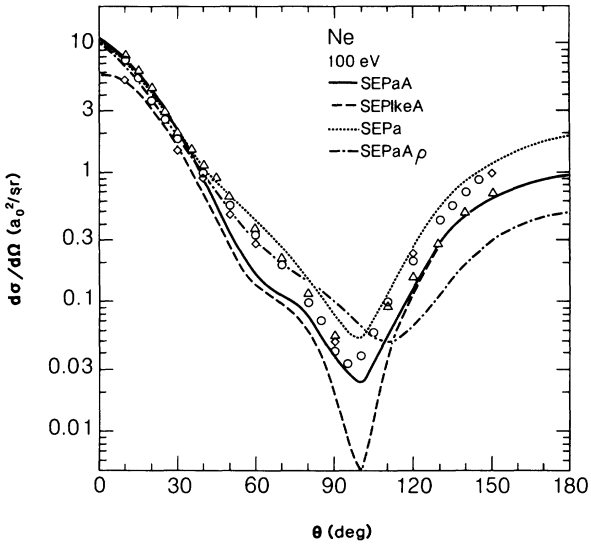

FIG. 12. Same as Fig. 3 except for Ne at 100 eV.

We next consider σ_{abs} in Tables III and IV. The central issue of this study is the following: How well does the quasifree-scattering model with Pauli blocking predict σ_{abs}? The answer given by Tables III and IV is as follows: reasonably well over a wide range of energy. For He the nonempirical calculated σ_{abs} values agree with the experimental values to 16% or better at 50–400 eV and underestimate the experimental values by 27% and 38% at 1000 and 3000 eV. For Ne the nonempirical calculated σ_{abs} are systematically higher than the experimental values with the overestimation factor in the relatively narrow interval of 1.42–1.73 over the whole 30–3000 eV range. To learn whether this represents a trend whereby the model becomes worse for targets with more electrons or heavier nuclei we applied the model to Ar; this study will be published elsewhere[41,42] but we note that the agreement between the calculated and experimental[20] σ_{abs} values for Ar is even better than that found here for He. This makes us suspect that the experimental values may be systematically low for Ne; however the matrix-effective-potential calculations that we reported previously are only slightly

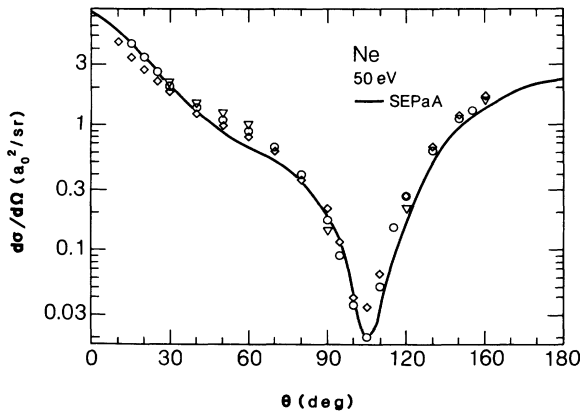

FIG. 11. Same as Fig. 3 except for Ne at 50 eV.

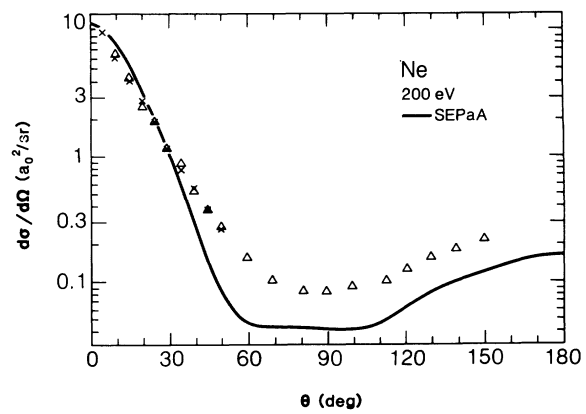

FIG. 13. Same as Fig. 3 except for Ne at 200 eV.

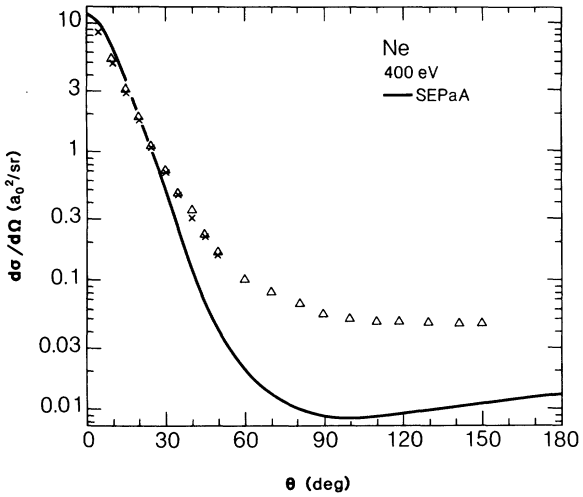

FIG. 14. Same as Fig. 3 except for Ne at 400 eV.

less accurate for Ne than He,[16,24,40] so the amount of systematic error in the experiment is probably not large. If we discount the possible experimental error, then we conclude that the accuracy of the present model does not vary montonically with target size for the rare gases. Further work to confirm or improve the experimental values of σ_{abs} for Ne would be very welcome. In any event it is encouraging that the calculated σ_{abs} values have the same energy dependence as the experimental ones for Ne. For He, the calculated σ_{abs} values are relatively low at 30 eV and as already mentioned, at 1000—3000 eV.

Finally, we consider the large-angle elastic scattering cross sections. For He the agreement with experiment is excellent at 30 and 50 eV (Figs. 3 and 4) and somewhat worse but still good at 100—800 eV (Figs. 5—7 and Table V). At 1000—3000 eV the agreement with the experimental differential cross sections is excellent but the latter are available only for $\theta \leq 50°$. For Ne the best agreement between theory and experiment is for 50, 100, and 3000 eV with worse agreement at 30, 200, 400, and 1000 eV. The elastic momentum-transfer cross sections are sensitive to the large-angle scattering, and the comparisons of these values to experiment in Tables III and IV provides another test of the calculated cross sections for large-angle elastic scattering. The agreement is within 22% for He at 30—200 eV and for Ne at 30—100 eV. However the momentum-transfer cross sections are more severely underestimated (factors of 1.8 and 3.4) for Ne at 200 and 400 eV.

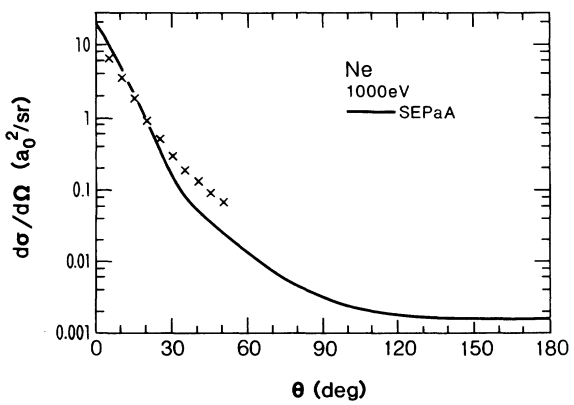

FIG. 15. Same as Fig. 3 except for Ne at 1000 eV.

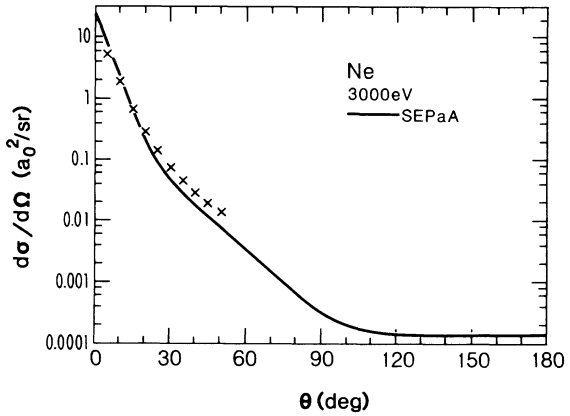

FIG. 16. Same as Fig. 3 except for Ne at 3000 eV.

VI. CONCLUDING REMARKS

We have proposed a nonempirical model for the absorption potential and have tested it thoroughly: in this article for two targets and over a range of two orders of magnitude of impact energies, and in a previous report[42] for Ar over the same energy range. Over the energy range 50—1000 eV the rms relative deviation of the calculated absorption cross sections from experiment is 15% for He and 57% for Ne. Over the full 30—3000-eV range the rms relative deviation is 28% for He and again 57% for Ne. The agreement with experiment for the differential cross sections is not consistent. In some cases it is excellent but there seems to be a trend to somewhat underestimate the large-angle elastic scattering especially at high energy.

It is interesting to compare the present approach to several previous approaches to calculate σ_{abs} and absorption effects on $d\sigma_{el}/d\Omega$ nonempirically.

Garrett and coworkers[43] have developed a complex optical potential approach and have applied it to e^--H scattering. Their approach involves a nonlocal complex potential for the elastic-channel optical potential whereas our work, both here and previously,[40,44] has been aimed at developing useful local forms for the optical potential.

McCarthy, Stelbovics, and Saha[45] have developed an approximation scheme for the complex optical potential in momentum space and a convenient equivalent local potential in coordinate space. Their method is based on explicit consideration of the discrete-state and continuum-state contributions to the optical potential, whereas the present approach uses no information about the excited wave functions of the target. An advantage of their method is that it is extendable to calculations of coupled channels plus the optical potential. As for the method discussed in the previous paragraph, this method has been applied only to e^--H scattering, so no numerical comparisons to the present results are possible.

The eikonal optical model has been applied to He, Ne, and Ar by Byron and Joachain.[36,47] For He it overestimates σ_{abs} by factors of 1.9 and 1.4 at 100 and 200 eV, respectively, and for Ne it overestimates σ_{abs} by factors of 2.7 and 1.8 at the same two energies;[36] these errors are much larger than those obtained with the present model. For Ar the same version of the optical eikonal model has a 28% rms error for 100–1000-eV energy range,[47] as compared to 8% for the present method over the same energy range.[42] It does appear, however, that the eikonal optical model gives more accurate differential cross sections at high energy and large scattering angles. A major disadvantage of the eikonal optical model is the difficulty in evaluating the expression for the absorption potential; a numerical integral is required even for atomic targets. In contrast, the present model reduces to a universal functional of target electron density, and this functional is equally as applicable to molecules as to atoms.

Another approach to σ_{abs} is the dispersion-equation approach employed by Valone and two of the authors.[40,44] In this approach the absorption potential is obtained by solving a principal-value integral equation involving the energy-dependent polarization potential as a function of impact energy. To be accurate over a wide energy range this theory requires knowing the polarization potential over a wide energy range. Also it is not clear with what accuracy the dispersion equation applies to localized model potentials. Further testing is underway in our laboratory to try to determine which of the following three approaches is most accurate: (i) model V^P directly and use the dispersion equation to calculate V^A as in Ref. 44; (ii) model V^A directly, for example by an empirical approach[37,48] or by the present model, and use the dispersion equation to calculate V^P; or (iii) model both V^P and V^A directly, as in the present paper. The development of a successful nonempirical model for V^A, as attempted here, is of course a necessary first step for nonempirical approaches of types (ii) and (iii).

Another approach to calculating σ_{abs} is the matrix-effective-potential (MEP) method.[16,24,39,40,49] This method does not require an accurate energy-dependent polarization potential as input but rather an accurate adiabatic polarization potential, which is easier to obtain. It involves only real potentials but it requires explicit treatment of an electronically excited pseudochannel. It does not require any free-electron approximations, and so it is, in principle, less approximate. For He the rms relative error in σ_{abs} is 11% for 50–400 eV or 19% for 30–400 eV.[16] For Ne the rms relative error is 37% for 50–700 eV but a factor of 2.8 at the near-threshold energy of 30 eV.[24,39] As compared to the present model, the MEP method is less accurate for Ne at 30 and 50 eV, about the same for He at 50 eV and above, and more accurate for He at 30 eV and for Ne at 100 eV and above. Above 100 eV the MEP also appears to give more accurate elastic momentum-transfer cross sections and elastic differential cross sections at large scattering angles[24,40] than either the eikonal optical model or the present model. Thus, at the computational expense of treating two coupled electronic channels instead of one, the MEP appears to be a more accurate way to treat absorption effects above 100 eV. Nevertheless, a single-channel complex potential has important interpretive advantages, and we are encouraged by the success of the present very simple model for calculating such a potential nonempirically.

A brief communication of parts of the present work has been published elsewhere[41] and an application to Ar will appear in a symposium proceedings.[42] The present paper presents the derivation and our first complete discussion of the quasifree-scattering model, plus the results for He and Ne over a very wide energy range. The overall conclusion of the study is that the simple binary-collision model with Pauli blocking is remarkably successful for the absorption cross sections over the whole energy range and for the differential elastic cross sections at 50–100 eV. The high-energy, large-angle differential elastic cross sections, which are very small, are underestimated.

ACKNOWLEDGMENT

This work was supported in part by the National Science Foundation through Grant No. CHE-80-25232.

APPENDIX

The Strand-Bonham fits for $\rho(r)$ fail for very small r, where the use of the tabulated constants from their paper leads to inaccurate values due to the inexact cancellation of terms. In particular, for $\rho(0)$ to be finite it is required that

$$\sum_i {}^a\gamma_i {}^a\lambda_i^2 - 2\sum_j {}^b\gamma_j {}^b\lambda_j = 0 \,. \tag{A1}$$

For He, we forced (A1) to be satisfied by changing their constant ${}^a\lambda_1$ from 2.4907 to 2.490 795 656, and for Ne we replaced $\rho(r)$ by $\rho(2\times10^{-3}\,a_0)$ whenever $r \le 2\times10^{-3}\,a_0$. With these modifications, $\rho(0)$ for He and Ne are 3.5991 and 604.04 a.u., respectively. For comparison, the Hartree-Fock values of $\rho(0)$ obtained from the tabulation of Fraga *et al.*[50] are 3.5959 and 619.90 a.u. for He and Ne, respectively. The (13,9,3) Gaussian basis of Douglass *et al.*[15] yields $\rho(0)=604.04$ a.u.

If (A1) is satisfied, then the density at the origin is given by

$$\rho(0) = \frac{Z}{4\pi}\left[3\sum_j {}^b\gamma_j {}^b\lambda_j^2 - \sum_i {}^a\gamma_i {}^a\lambda_i^3\right] . \tag{A2}$$

It is possible to adjust the Strand-Bonham fits to give an accurate value of $\rho(0)$, when one is known, by adjusting two of their constants to simultaneously satisfy (A1) and (A2). This was not done for the present calculations because it would have had a negligible effect on the results.

*Present address: Department of Chemistry, Columbia University, New York, NY 10027.
[1]R. Serber, Phys. Rev. 72, 1114 (1947).
[2]M. L. Goldberger, Phys. Rev. 74, 1269 (1948).
[3]E. Clementel and C Villi, Nuovo Cimento 2, 176 (1955).
[4]G. F. Chew and G. C. Wick, Phys. Rev. 85, 636 (1952).
[5]G. Takeda and K. M. Watson, Phys. Rev. 94, 1087 (1954); 97, 1336 (1955).
[6]B. Sinha, Phys. Rep. C 20, 1 (1975).
[7]S. Fernbach, W. Heckrotte, and J. V. Lepore, Phys. Rev. 97, 1059 (1955).
[8]L. I. Schiff, *Quantum Mechanics,* 3rd ed. (McGraw-Hill, New York, 1968), p. 130.
[9]G. E. Brown, Proc. Phys. Soc. London, Sect. A 70, 361 (1957).
[10]L. R. B. Elton, Nucl. Phys. 23, 681 (1961).
[11]C. J. Joachain, *Quantum Collision Theory* (North-Holland, Amsterdam, 1975), pp. 156–159.
[12]D. G. Truhlar, in *Chemical Applications of Atomic and Molecular Electrostatic Potentials,* edited by P. Politzer and D. G. Truhlar (Plenum, New York, 1981), p. 123.
[13]M. E. Riley and D. G. Truhlar, J. Chem. Phys. 63, 2182 (1975).
[14]T. G. Strand and R. A. Bonham, J. Chem. Phys. 40, 1686 (1964).
[15]C. H. Douglass, Jr., D. A. Weil, P. A. Charlier, R. A. Eades, D. G. Truhlar, and D. A. Dixon, in *Chemical Applications of Atomic and Molecular Electrostatic Potentials,* edited by P. Politzer and D. G. Truhlar (Plenum, New York, 1981), p. 173.
[16]D. Thirumalai, D. G. Truhlar, M. A. Brandt, R. A. Eades, and D. A. Dixon, Phys. Rev. A 25, 2946 (1982).
[17]D. G. Truhlar, D. A. Dixon, and R. A. Eades, J. Phys. B 12, 1913 (1979).
[18]S. M. Valone, D. G. Truhlar, and D. Thirumalai, Phys. Rev. A 25, 3003 (1982).
[19]F. J. deHeer and R. H. J. Jansen, J. Phys. B 10, 3741 (1977).
[20]F. J. deHeer, R. H. J. Jansen, and W. van der Kaay, J. Phys. B 12, 979 (1979).
[21]C. E. Moore, *Atomic Energy Levels* (National Bureau of Standards, Washington, 1949), Vol. I.
[22]D. Thirumalai and D. G. Truhlar, Phys. Rev. A 27, 158 (1983).
[23]M. A. Brandt, M. S. thesis, University of Minnesota, Minneapolis, 1975 (unpublished).
[24]D. Thirumalai and D. G. Truhlar, Phys. Rev. A 25, 3058 (1982).
[25]T. F. O'Malley, L. Spruch, and L. Rosenberg, J. Math. Phys. 2, 491 (1961).
[26]D. F. Register, S. Trajmar, and S. K. Srivastava, Phys. Rev. A 21, 1134 (1980).
[27]R. H. J. Jansen, F. J. deHeer, H. J. Luyken, B. van Wingerden, and H. J. Blaauw, J. Phys. B 9, 185 (1976).
[28]S. C. Gupta and J. A. Rees, J. Phys. B 8, 417 (1975). The momentum-transfer cross sections from this reference are the recomputed values of Refs. 24 and 40.
[29]D. F. Register and S. Trajmar, Phys. Rev. A (in press).
[30]T. W. Shyn, Phys. Rev. A 22, 916 (1980).
[31]G. B. Crooks, Ph.D. thesis, University of Nebraska, Lincoln, 1972 (unpublished).
[32]M. V. Kurepa and L. Vušković, J. Phys. B 8, 2067 (1975).
[33]J. F. Williams and A. Crowe, J. Phys. B 8, 2233 (1975).
[34]R. D. DuBois and M. E. Rudd, J. Phys. B 9, 2657 (1976).
[35]J. B. Furness and I. E. McCarthy, J. Phys. B 6, 2280 (1973).
[36]F. W. Byron, Jr., and C. J. Joachain, Phys. Rev. A 15, 128 (1977).
[37]A. E. S. Green, D. E. Rio, and T. Ueda, Phys. Rev. A 24, 3010 (1981).
[38]I. E. McCarthy, C. J. Noble, B. A. Phillips, and A. D. Turnbull, Phys. Rev. A 15, 2173 (1977).
[39]K. Onda and D. G. Truhlar, Phys. Rev. A 22, 86 (1980).
[40]D. Thirumalai and D. G. Truhlar, Phys. Rev. A 26, 793 (1982); 28, 3140(E) (1983).
[41]G. Staszewska, D. W. Schwenke, D. Thirumalai, and D. G. Truhlar, J. Phys. B 16, L281 (1983).
[42]G. Staszewska, D.W. Schwenke, and D. G. Truhlar, Int. J. Quantum Chem. Symp. (in press).
[43]G. D. Alton, W. R. Garrett, M. Reeves, and J. E. Turner, Phys. Rev. A 6, 2138 (1972); P. W. Coulter and W. R. Garrett, *ibid.* 18, 1902 (1978); 23, 2213 (1981).
[44]S. M. Valone, D. Thirumalai, and D. G. Truhlar, Int. J. Quantum Chem. Symp. 15, 341 (1981).
[45]I. E. McCarthy, and A. T. Stelbovics, Phys. Rev. A 22, 502 (1980); I. E. McCarthy, B. C. Saha, and A. T. Stelbovics, *ibid.* 23, 145 (1981); Aust. J. Phys. 34, 135 (1981); J. Phys. B 14, 2871 (1981); 15, L401 (1982).
[46]I. E. McCarthy and A. T. Stelbovics, J. Phys. B 16, 1233 (1983).
[47]C. J. Joachain, R. Vanderpoorten, K. H. Winters, and F. W. Byron, Jr., J. Phys. B 10, 227 (1977).
[48]G. Staszewska, D. W. Schwenke, and D. G. Truhlar, Phys. Rev. A 28, 169 (1983).
[49]D. G. Truhlar and K. Onda, Phys. Lett. 76A, 119 (1980).
[50]S. Fraga, J. Karwowski, and K. M. S. Saxena, *Handbook of Atomic Data* (Elsevier, Amsterdam, 1976).